DOI: https://doi.org/10.37434/tpwj2023.09.05

THERMAL PROCESSES AND EVOLUTION OF STAINLESS STEEL STRUCTURE IN FRICTION STIR WELDING WITH A TOOL FROM pcBN

A.L. Maistrenko[1], M.P. Bezhenar[1], S.D. Zabolotnyi[1], V.A. Dutka[1], M.O. Cherviakov[2], A.M. Stepanets[1], I.O. Gnatenko[1], M.O. Tsysar[1]

[1]V. Bakul Institute for Superhard Materials of the NASU
2 Avtozavodska Str., 04074, Kyiv, Ukraine
[2]E.O. Paton Electric Welding Institute of the NASU
11 Kazymyr Malevych Str., 03150, Kyiv, Ukraine

ABSTRACT

It is shown that application of superhard materials based on cubic boron nitride for manufacture of working components of the tool for realization of friction stir welding processes allows ensuring the tool thermomechanical resistance. Computer modeling of the temperature field in the tool, and in steel parts during friction stir welding of stainless steels with a tool based on polycrystalline boron nitride (pcBN) was performed. Agreement between the numerical and experimental results of temperature distribution in the tool movement zone is shown. Strength of welded joints of stainless steel parts was determined, and evolution of weld structure was analysed.

KEYWORDS: structure evolution, friction stir welding, tool, kiborit, strength, modeling, stainless steels, temperature field

INTRODUCTION

As is known, the process of friction stir welding (FSW) is conducted at temperatures much lower than melting temperature of the metals and alloys being welded. It results in an essential lowering of residual stresses and temperature deformations, and evolution of the joint zone microstructure takes place that has a positive influence on ensuring the part material strength in their joint zone. Initially, this method was successfully used for welding magnesium- and aluminium-based alloys [1]. Magnesium alloys turned out to be a material readily weldable by FSW method, as the welding process is conducted at low temperatures (200–260 °C) with application of steel tools [1–3]. In friction stir welding of aluminium alloys the observed characteristic temperatures in the welding zone were in the range of 300–400 °C. Realization of the process of FSW of copper-based materials is performed already at temperatures of 600–700 °C that requires application of hard-alloy tools [4]. For welding steels and high-temperature alloys, however, in welding of which the temperature of 600–1000 °C is observed, a tool with already much higher thermomechanical resistance is required, in particular, based on special hard alloys or polycrystalline materials based on cBN [5, 6]. In order to substantiate the optimal design of the tool and produce a sound welded joint of the parts, as a result of FSW, it is rational to first of all perform mathematical modeling of the thermal state of the tool and the parts during welding [5–7].

Over the last twenty years, FSW method has been used for welding heat-resistant steels and alloys. Realisation of the process of FSW of stainless steels of austenitic-ferritic type and high-temperature alloys requires application of a tool from heat-resistant materials, which include special hard alloys and polycrystalline materials based on cubic boron nitride (pcBN) [8, 9].

V. Bakul Institute for Superhard Materials of the NASU is working on development and application of tools for FSW for different metals and alloys [1–4, 7]. Here, the properties of materials used for tool manufacture, should be much higher than the mechanical characteristics of the materials being welded or surfaced. More over, the tool, particularly, its working part (pin), should preserve a high wear resistance and heat resistance at high temperatures. These materials should retain their properties at rather high temperatures and cyclic loads, which are due to the forces applied to the tool during circular bending in welding or surfacing.

The objective of the work is to develop a tool from polycrystalline boron nitride (pcBN) for friction stir welding of stainless steels, analysis of thermal processes in welding and evaluation of the mechanical characteristics of the welded joints.

MATERIALS AND INVESTIGATION PROCEDURES

Polycrystalline superhard materials based on cBN are known in the world market as tool pcBN materials. The tendencies in development of studies in the field of creation of polycrystalline superhard materials based on CBN can be illustrated in the case of products of a number of foreign firms, in particular Element Six and MegaDiamond Companies [10, 11]. In Kiborit material of this class [8, 9], where the main phase is cBN (about

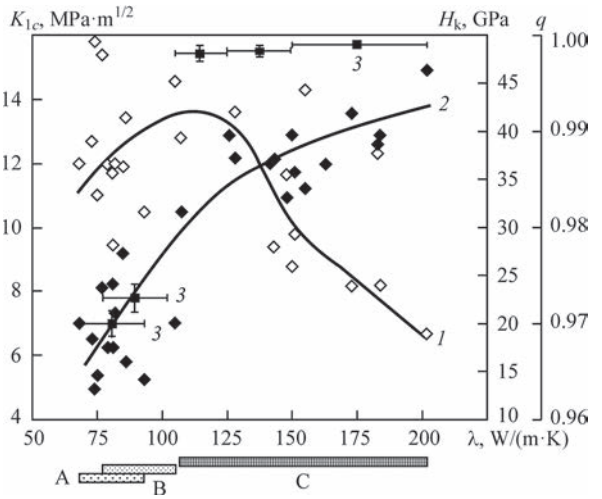

Figure 1. Crack resistance (*1*), hardness (*2*) and relative density (*3*) of polycrystals obtained by reaction sintering of CBN powder with 2 wt.% Al [9]

84 %), which is a determinant factor for formation of the structure of a composite material with a continuous frame and high hardness. Kiborit of all the grades is produced by reaction sintering of cBN with Al under high pressure conditions in hard-alloy high-pressure apparatuses (HHA) of "anvil with recess" design of "toroid" type [8, 9]. Special features of the properties of pcBN-based composites consist in their high hardness and crack resistance, chemical resistance and predominantly tribochemical wear mechanism. In the first case, there is more than 80 % cBN in the material composition, hardness is ensured by cBN frame, and crack resistance is high due to the binder along the grain boundaries (Table 1) [9]. Materials with more than 95 % cBN content in the structure have higher hardness. An example of such a material is Kiborit-1, developed at ISM of the NASU. A feature of the structure is absence of a continuous binding frame (binder composition is AlN and AlB_{12}, quantity is 3 wt.%; it is arranged in the form of inclusions along the grain boundaries). Kiborit-2 material — pcBN is produced by the method of preimpregnation of compacted cBN powder by aluminium with subsequent reaction sintering at a high pressure [8, 9]. Sintering parameters of Kiborit-2 material are as follows temperature of 1600–1750 K and pressure of up to 4.5 GPa. Here, additional evolution of the energy of chemical reaction in the working volume, alongside the external heating energy, should be noted. For such a process, steel HHA are the best, [12], one of the advantages of which is the large working volume, allowing production of large-sized samples of 32 mm diameter and 15 mm height in presses with 20 MN force (Table 2).

Table 1. Physico-mechanical properties of some Kiborit grades [9]

Characteristics	Kiborit-1	Kiborit-2	Kiborit-3
CBN quantity, %	96–97	84	70–75
Specific weight, g/cm^3	3.40–3.45	3.35–3.38	3.60
Knoop hardness at 10 N load, GPa	32–36	28–30	27
Crack resistance K_{1c}, MPa·m$^{1/2}$	8–13.5	10.5	10.5
Compressive strength, GPa	3.2	2.9	2.9
Tensile strength, GPa	0.37	-	-
Modulus of elasticity, *E*, GPa	880	-	-
Poisson's ratio	0.16		
Heat conductivity λ, W/(m·K)	150	70	70
Heat resistance up to temperature, K	1400	1400	1400
Resistance to oxidation in air to temperature, K	1200	1200	1200
TEC, $\alpha \cdot 10^{-6}$ K^{-1}	–	4.9–7.9	–
Plate diameter, mm	6.35–12.7	9.6–31.8	9.6–31.8

Figure 1 shows the changes in relative density (ρ), hardness (*H*k) and crack resistance (K_{Ic}) in polycrystalline materials of the considered type for three groups (A, B, C) [9].

New Kiborit application is the work tool for friction stir welding. Rotating tools of this type consist of a shoulder and protruding pin — Figure 2. In welding the pin is immersed into the blank, and the shoulder is pressed to the surface. Friction at tool rotation generates heat, which is sufficient for transition of the materials being joined into an elasto-plastic state.

Kiborit-1 was produced by reaction sintering of cubic boron nitride powder (up to 98 %) with aluminium [8, 9]. Presence of other additives in the charge and high sintering parameters led to obtaining in the composition of Kiborit-1 binder also higher β-AlB_{12} boride, alongside AlN and AlB_2. A combination of high hardness Hk (36–38 GPa) and high heat conductivity (100–150) W/m·K with sufficiently high level of crack resistance (≥ 8 MPa·m$^{1/2}$) of Kiborit-1 enabled

Table 2. Mechanical properties of the studied materials [13]

Steel	*E*, GPa	$\sigma_{0.2}$, MPa	σ_t, MPa	δ, %	T_m, °C
08Kh18N10T (AISI 321 analog)	193	196	470	40	1400–1455
AISI 304 (08Kh18N10 analog)	196	205	510	40	1400–1455
EP-718 (KhN45MVTYuBR) (acc.to TU 14-1-3905-85)	205	550	1240	30	1260–1336
EI 698 (Kh73MBTYu)	200	705	1150	16	1370–1400

its application in blade tools. Development of superhard polycrystalline Kiborit-2 material is based on the principles of creation of a material with a continuous structure of CBN frame and reaction sintering with aluminium. The difference consisted in such a control of sintering parameters, which ensured increase of "CBN–another phase" contact surface at preservation of continuous CBN frame in the structure [9]. The given results show that hardness of the real polycrystals, containing from 65 to 96 % CBN and AlN-based binder, in all the cases is somewhat lower than the calculated one in the assumption of additive dependence on the phase composition.

Thus, we have the possibility of choosing from the composites of Kiborit series an appropriate material for application in the tools for friction stir welding of steels. It was exactly Kiborit-2, which was selected for tool manufacture, based on its high heat-resistance (1200 °C), as well as because this material has maximal crack resistance K_{1c} = 10.5 MPa·m$^{1/2}$, which is important at cyclic circular bending of the pin, and diameter and height dimensions of the blank of 32×15 mm, which allowed manufacturing tools with pin height of 5–6 mm and should diameter of 25 mm (Figure 2, *a*).

Stainless steels of AISI type (08Kh18N10 analog), 08Kh18N10T (AISI 321 analog), 03Kh20N16AG6, 02Kh18MBV and heat-resistant EP-718 (KhN45MVTYuBR) and EI-698 (KhN73MBTYu) alloys [13]. Mechanical properties of some of them are given in Table 2. Figure 2, *b* shows the appearance of the weld in welding AISI 304 steel.

MEASURING THE FORCE COMPONENTS IN WELDING OF STEELS

Investigations on friction stir welding of steels with measurement of the components of the force acting on the tool, were performed in the bench mounted on the table of vertical milling machine 654, fitted with measuring sensors and software of HBM Company (Figure 3). Welding modes: tool rotation speed of 800 rpm^{-1} and feed rate of 20–50 mm/min. The tool is mounted at 88° angle relative to the part surface. Samples of 3–4 mm thickness were studied (Table 3). Welding of the studied steel samples was performed in a special bench, fitted with a system of sensors, which measure the vertical and shear components of the force, applied to the end effector (Figure 3, Table 3). It is found that the average force components, irrespective of the rotation frequency and speed of welding with the tool with the conical pin stay on the same level for all the studied steel samples of the same thickness (Table 2).

TEMPERATURE MEASUREMENT IN THE WELDING ZONE

Temperature measurement in the welding zone was performed with an infrared imager Fluke-ir25 with 5 s

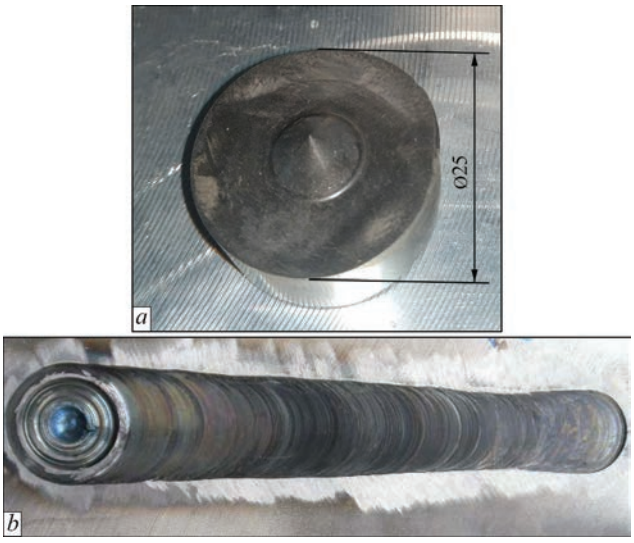

Figure 2. General view of the tool from polycrystalline boron nitride for welding stainless steels (*a*) and general view of the weld in AISI 304 steel welding (*b*)

resolution at different moments of the tool movement along the sample (Figure 4).

TEMPERATURE FIELD MODELING AT FSW OF STAINLESS STEELS

Mathematical modeling of the temperature field in the parts being welded during FSW was performed. A 3D stationary model was selected, which is based on a nonlinear equation of heat conductivity. Redistribution of heat sources over the surfaces of the tool pin contact with the parts being welded is taken into

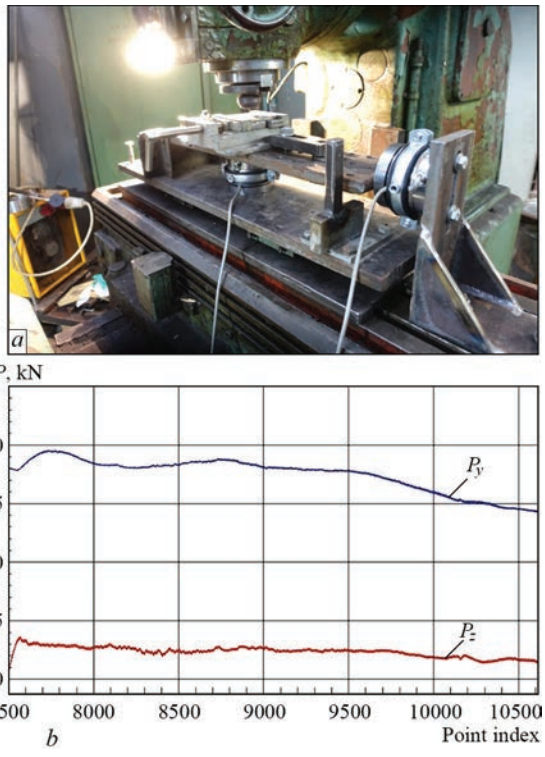

Figure 3. General view of a bench for studying the process of friction stir welding of steels (*a*), graph of the change of the components of a force acting on the tool (*b*)

Table 3. Results of measuring the force components (FSW) of samples of the studied stainless steels

Sample material	Sample thickness, mm	Horizontal component P_z, N		Vertical component P_y, N	
		Average	max	Average	max
03Kh20N16AG6	4	2385	3423	17597	19545
AISI 304 (08Kh18N10 analog)	3	1226	2766	11992	15780

account. Heat exchange with ambient air on the part free surfaces is also allowed for.

The material of the parts being welded is AISI 304 stainless steel. Two plates of 200×100×3 (4) mm size were welded by FSW along the plate larger size. The welding tools were made from Kiborit-2 material. Temperature dependencies of thermophysical properties of AISI 304 steel on temperature were taken into account: heat capacity C_p, thermal conductivity coefficient λ, density ρ, yield limit σ_y [14–16].

MATHEMATICAL MODEL OF THE TEMPERATURE FIELD

A stationary mathematical model was considered for description of the temperature field in FSW zone [17]:

$$C_p\rho(\vec{u}\ \mathrm{grad}\,T) = \mathrm{div}(\lambda\ \mathrm{grad}\,T), \quad (1)$$

where T is the temperature; C_p, ρ, λ are the specific heat capacity, density and thermal conductivity coefficient, respectively; $\vec{u}$ is the vector of the speed of the part forward movement relative to the tool.

Respective boundary conditions are assigned on the surfaces of the tool and parts (plates), as well as on the surface of contact of the tool and the plates. Heat sources act on the surface of contact of the pin, shoulder and plates, which are due to friction and plastic deformation of the plate material in this contact zone.

Heat sources due to friction are active on the shoulder contact surface. The capacity of these heat sources is calculated by the following formula

$$q_s = \begin{cases} \dfrac{2\pi r n \mu F}{A_s}, \text{ at } T < T_m, \\ 0, \text{ at } T \geq T_m, \end{cases} \quad (2)$$

where r is the distance from a point of this contact surface to the axis of rotation of the shoulder with the pin; n is the number of shoulder rotations per minute; μ is the friction coefficient; F is the axial force, acting on the pin with the shoulder; A_s is the area of the surface of shoulder contact with the parts; T_m is the temperature of plate material melting.

Figure 5 shows the results of calculations of temperature distributions in the components of the tool structure and AISI 304 steel plate being welded. Figure 6 gives a comparison of experimental and calculated temperatures. The given maximal values of experimentally measured temperatures are unfortunately limited by instrument characteristics and difficult access of the instrument to the welding zone, but it means that these are not the maximal acting temperatures in the welding zone, just acting maximal temperatures in the measured (limited) section.

INVESTIGATION RESULTS AND THEIR DISCUSSION

Experimental determination of temperature distribution in the welding zone of the studied steels was conducted. Results of temperature distributions in the measured welding zones of the studied steels beyond the tool shoulder are given in Figure 7.

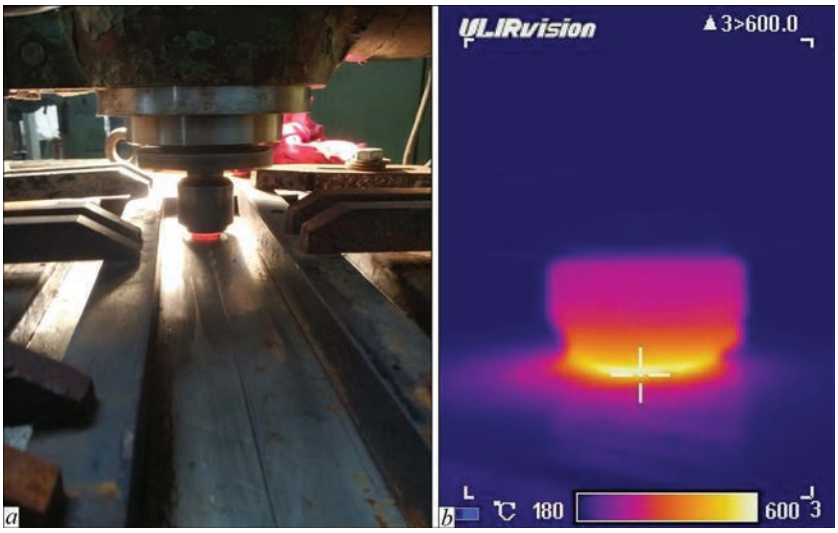

Figure 4. Images of FSW of 3 mm plates from AISI 304 steel (*a*), measurement of temperature distribution at FSW of stainless steel (beyond the tool shoulder) (*c*)

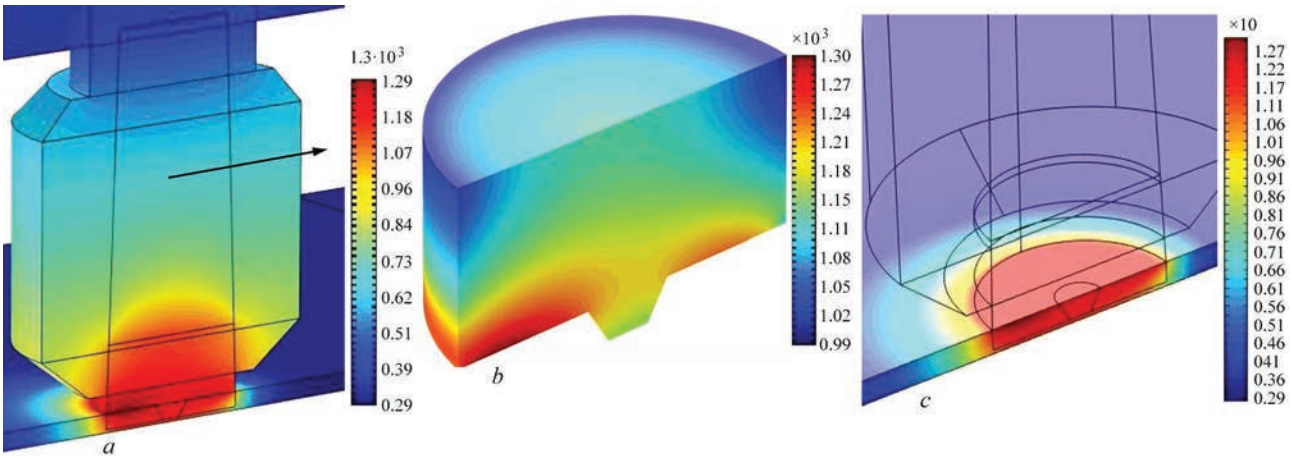

Figure 5. Pattern of the temperature field calculated in different parts of the computational domain (maximal temperature — 1303 K): *a* — in the plate, tool and tool fixtures (arrows show the direction of the tool forward movement); *b* — in the tool; *c* — in the plate being welded

Maximal studied temperature of welding the steel samples varied from 500 to 800 °C (Figure 7), temperature of welding 4 mm thick samples being practically 1.5 times higher than that of 3 mm samples, which is due to greater work of plastic deformations in the welding zone. Note also that the average temperature in welding of the studied steels is equal to T_{av} = 712 °C, i.e. the mean temperature of welding steels of austenitic-ferritic class corresponds to equation T_w = (0.45–0.62) T_m, unlike the known temperature range of welding magnesium and aluminium alloys, which corresponds to T_w (0.4–0.5)T_m ratio.

Metallographic investigations of welded samples were performed on polished microsections etched in $HCl + HNO_3$ solution for 5 min. Microstructure images obtained in optical microscope XUM-102 at ×500 magnification are shown in Figure 8. Individual grain sizes were determined using LevenhukLite software, and they are given directly in the images.

In welding 08Kh18N10T steel, the grain size practically does not change, as the size of individual grains in the welding zone is in the range of 10–20 μm, and in the initial metal it is 5–15 μm. Grain size in the welding zone of 02Kh18MBV steel is 10–50 μm, and in the material being welded it is 50–150 μm, i.e. grain size in the weld is reduced relative to the initial metal by 3 to 5 times. Growth of individual grains is observed in the zone of welding 03Kh20N16AG6 steel. So, while in the base metal grain size is 2–10 μm, in the weld zone is increased to 10–50 μm. Grain size in weld metal of AISI 304 steel (08Kh18N10T) is 20–60 μm, and in the base metal grain size reaches 40–100 μm, i.e. in welding AISI steel grain size refinement by 1.6 to 2.0 times occurs in the welded joint zone.

Base on metallographic analysis of the change of grain size in the combined weld, the ratio of grain size in the weld of EP-718 alloy to grain size in the base metal decreases practically 2 times, and the size of

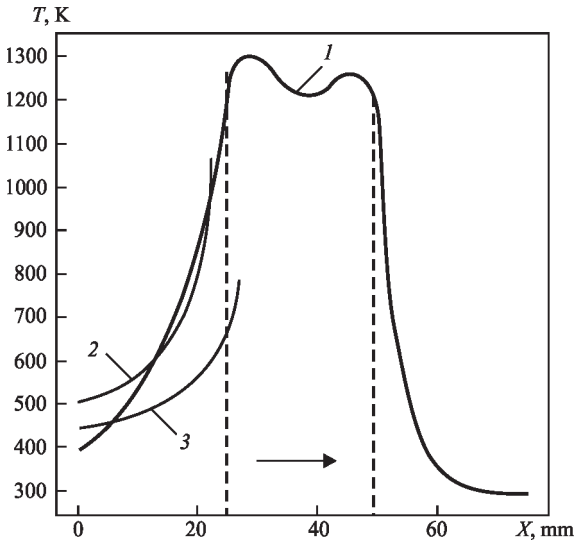

Figure 6. Comparison of calculated (*1*) and experimental (*2*, *3*) temperatures along the line of welding the steel plates. Coordinate *X*, mm is the scale bar of the welded steel sample. The arrow shows the direction of tool movement. Dashed lines are the tool shoulder limits (*2* — Kh18N10T steel — 4 mm; *3*— AISI 304 steel — 3 mm)

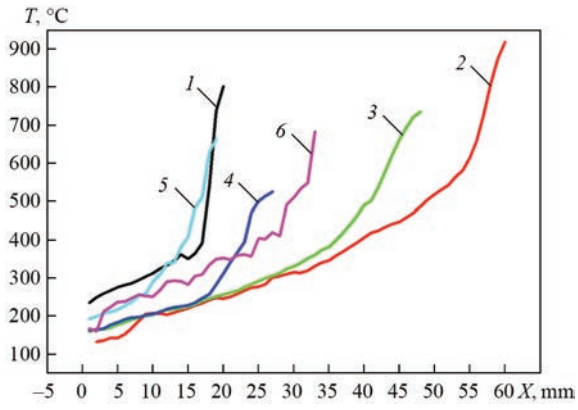

Figure 7. Experimentally determined temperature distributions behind the tool shoulder during FSW: thickness of 08Kh18N10T steel plate (*1*) — 4 mm; 02Kh18MBV steel (*2*) — 4 mm; 03Kh20N16AG6 steel (*3*) — 4 mm; AISI 304 steel (*4*) — 3 mm; EP-718 (*5*) — 4.3 mm; KhN73MBTYu steel (*b*) — 4.3 mm; *X* — coordinate is the scale bar of the steel sample being welded

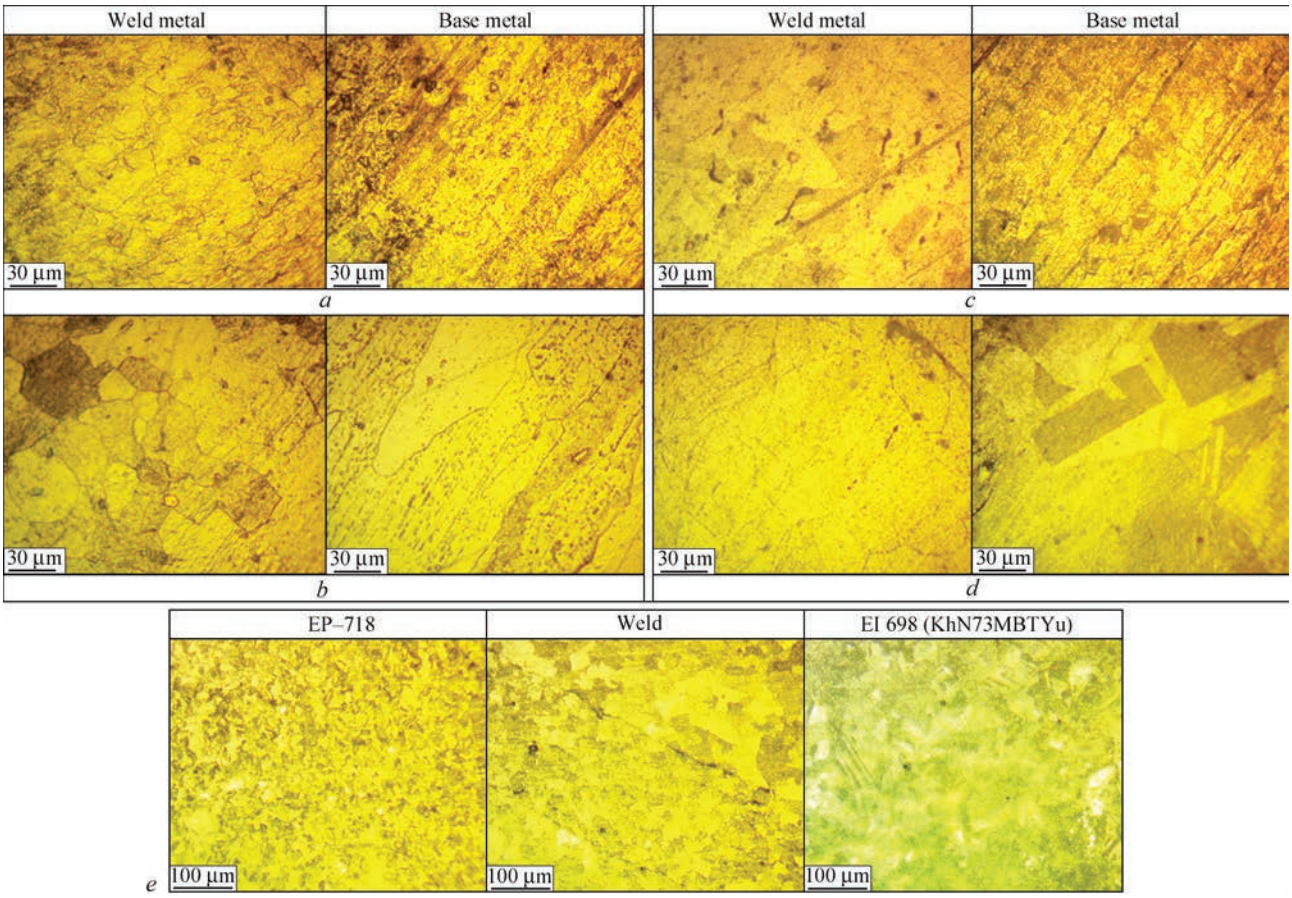

Figure 8. Evolution of weld structure in the studied steels (×500): 08Kh18N10T (*a*); 02Kh18MBV (*b*); 03Kh20N16AG6 (*c*); AISI 304 — 08Kh18N10 steel analog (*d*), EP 718 — EI 698 (*e*)

Table 4. Strength of the studied steels in the initial state and of their welded joints

Матеріал	Sample type	σ_y, MPa	σ_t, MPa	$\sigma_t^з/\sigma_t^о$
08Kh18N10T	Base metal	194	474	–
	Welded joint	135	280	0.59
02Kh18MBV	Base metal	429	707	–
	Welded joint	183	385	0.54
03Kh20N16AG6	Base metal	403	758	–
	Welded joint	275	390	0.51
AISI 304	Base metal	202	511	–
	Welded joint	171	349	0.68

grains in EI 698 steel weld is reduced 3 times relative to grain sizes in the base metal.

STRENGTH OF FSW JOINTS OF THE STUDIED STEELS

Tensile testing of material welded samples was performed in servohydraulic machine MTS-318.25. All the samples of the studied metals for strength determination were cut out in one direction — orthogonally to the welded plate axis. Strength of the studied steel welded joints relative to that of base metal of these steels was determined. It should be noted that the ratio of welded joint to base metal strength varied in the range from 0.51 to 0.68 (Table 4), i.e. strength lowering is quite significant, which determines the need to optimize the kinematic and force parameters of FSW process, which will ensure higher strength of the welded joints. Therefore, optimization of kinematic and force parameters of the welding process, which should ensure the high strength of the welded joint, requires a long and careful research, which is the next goal in the development of this area of technology.

CONCLUSIONS

1. A tool from polycrystalline boron nitride (pcBN) was developed for FSW of stainless steels and high-temperature nickel alloys. Test tools were manufactured from pcBN Kiborit-2 for realization of the process of FSW of structural components from up to 4 mm stainless steels and high-temperature alloys.

2. A model of the thermal process of friction stir welding of stainless steel was proposed and temperature distributions in the tool and parts being welded were calculated.

Investigations of thermal processes during welding showed that, depending on the thickness of samples being welded, the maximal temperature in the studied steel welding zone varied from 500 to 900 °C, which is approximately equal to $(0.45–0.62)T_m$.

3. A metallographic study was performed of the mean size of weld grain, compared to the sample base metal was performed. So, the mean size of grains in the zone of

welding 08Kh18N10T steel is in the range of 10–20 μm, and in the initial metal it is 5–15 μm, i.e. it remains without any significant changes. Mean size of grains in the welding zone of 02Kh18MBV steel reaches 10–50 μm, and in the weld material it is 50–150 μm, i.e. the grain size in the weld is reduced from 3 to 5 times relative to that of the base metal. In the zone of 03Kh20N16AG6 steel weld, a slight growth of the sizes to 10–50 μm is observed relative to the base metal with grain size of 2–10 μm. Grain size in the weld of AISI 304 steel reaches 20–60 μm, compared to base metal with grain size of 40–100 μm. Therefore, in welding a refinement of grain size from 1.6 to 2.0 times is found in the welded joint zone. Mean grain size in the weld of a mixed joint of EP-718 and EI-698 alloys is reduced from 2 to 3 times, relative to that of grains in the base meal of these alloys.

4. The ratio of strength of the studied material welded joints and that of the base metal varied in the range from 0.51 to 0.68, which determines the need to conduct more profound studies, aimed at optimization of FSW kinematic and force parameters, which will provide a higher strength of welded joints of this type.

REFERENCES

1. Majstrenko, A.L., Lukash, V.A., Zabolotny, S.D. et al. (2016) Application of friction stir method for welding of magnesium alloys and their structure modifying. *The Paton Welding J.*, **5–6**, 68–74. DOI: https:// doi.org/10.15407/tpwj2016.06.11
2. Maistrenko, A.L., Lukash, V.A., Usenko, B.O. et al. (2019) Welding of aluminium curvilinear panels by friction stir welding method. In: *Abstr. of Pap. of All-Ukrainian Int. Conf. on Problems of Welding and Related Technologies (17–19 September, 2019, Mykolaiv-Koblevo)*, 85–86.
3. Gnatenko, I.O., Oliinyk, N.O., Ilnytska, G.D. et al. (2019) Influence of friction stir welding on corrosion resistance of high-strength aluminium alloys. Rock destruction and metal-working tool: Technique and technology of its fabrication and application. Issue 22. Kyiv, ISM, 469–476 [in Russian].
4. Grigorenko, G.M., Adeeva, L.I., Tunik, A.Yu. et al. (2015) Application of friction stir welding method for repair and restoration of worn-out copper plates of MCCB moulds. *The Paton Welding J.*, **5–6**, 55–58.
5. Zhu, X.K., Chao, Y.J. (2004) Numerical simulation of transient temperature and residual stresses in friction stir welding of 304L stainless steel. *J. of Materials Proc. Technology*, **146**, 263–272.
6. Al-moussawi, M., Smith, A., Young, A. et al. (2016) An Advanced Numerical Model of Friction Stir Welding of DH36 Steel. In: *Proc. of 11th Inter. Symp. of Friction Stir Welding. Cambridge, UK.* https://www.researchgate.net/publication/305330065
7. Majstrenko, A.L., Nesterenkov, V.M., Dutka, V.A. et al. (2015) Modeling of heat processes for improvement of structure of metals and alloys by friction stir welding method. *The Paton Welding J.*, **1**, 2–10.
8. Novikov, M.V., Shulzhenko, O.O., Bezhenar, M.P. et al. (1998) *Method of sintering of composite material based on cubic boron nitride.* Pat. 25281A, Ukraine, Int. Cl. C04B35/5831. Fil. 21.07.97, Publ. 25.12.98 [in Ukrainian].
9. Novikov, N.V., Shulzhenko, O.O., Bezhenar, N.P. et al. (2001) Kiborit: Manufacture, structure, properties, application. *Sverkhtvyordye Materialy,* **2**, 40–51 [in Russian].
10. *Megadiamond pcBN Products for Industrial Tooling*. USA, The Publication of Megadiamond.
11. *Introduction to De Beers PCD and pcBN cutting tool materials*: 1.2.3. The Publication of De Beers Industrial Diamond Division.
12. Bezhenar, N.P., Romanenko, Ya.M., Konoval, S.M. et al. (2018) Kiborit: New materials and new fields of application. In: *Proc. of 6th Int. Samsonov Conf. on Materials Science of Refractory Compounds (Kyiv, Ukraine, 22–24 May 2018)*.
13. Zubchenko, A.S. (2003) Grades of steels and alloys. Moscow, Mashinostroenie [in Russian].
14. Bentz, D.P., Prasad, K. (2007) *Thermal Performance of Fire Resistive Materials I. Characterization with Respect to Thermal Performance Models*. Edition: NISTIR 7401. Publ., U.S. Department of Commerce.
15. Bentz, D.P., Flynn, D.R., Kim, J.H., Zarr, R.R. (2006) A slug calorimeter for evaluating the thermal performance of fire resistive materials. *Fire and Materials*, 30(**4**), 257–270.
16. Bogaard, R.H., Desai, P.D., Li, H.H., Ho, C.Y. (1993) Thermophysical properties of stainless steels. *Thermochimica Acta*, **218**, 373–393.
17. Nandan, R., Roy, G.G., Lienert, T.J., DebRoy, T. (2006) Numerical modelling of 3D plastic flow and heat transfer during friction stir welding of stainless steel. *Sci. and Technol. of Welding and Joining*, 11(**5**), 526–53.

ORCID

A.L. Maistrenko: 0000-0001-5479-326X,
S.D. Zabolotnyi: 0000-0003-1287-8454,
M.O. Cherviakov: 0000-0003-4440-7665,
I.O. Gnatenko: 0000-0002-9466-0215,
M.O. Tsysar: 0000-0002-4494-9109

CONFLICT OF INTEREST

The Authors declare no conflict of interest

CORRESPONDING AUTHOR

A.L. Maistrenko
E.O. Paton Electric Welding Institute of the NASU
11 Kazymyr Malevych Str., 03150, Kyiv, Ukraine.
E-mail: almaystrenko46@gmail.com

SUGGESTED CITATION

A.L. Maistrenko, M.P. Bezhenar, S.D. Zabolotnyi, V.A. Dutka, M.O. Cherviakov, A.M. Stepanets, I.O. Gnatenko, M.O. Tsysar (2023) Thermal processes and evolution of stainless steel structure in friction stir welding with a tool from pcBN. *The Paton Welding J.*, **9**, 31–37.

JOURNAL HOME PAGE

https://patonpublishinghouse.com/eng/journals/tpwj

Received: 28.06.2023
Accepted: 09.10.2023